Structural Analysis of the Additive Noise Impact on the α-tree

Baptiste Esteban[1 [0000−0002−6477−7666]], Guillaume Tochon[1 [0000−0003−4617−4922]], Edwin Carlinet[1 [0000−0001−5737−5266]], and Didier Verna[1 [0000−0002−6315−052X]]

EPITA Research Laboratory
14-16 rue Pasteur, Le Kremlin-Bicêtre, France
baptiste.esteban@lrde.epita.fr

Abstract. Hierarchical representations are very convenient tools when working with images. Among them, the α-tree is the basis of several powerful hierarchies used for various applications such as image simplification, object detection, or segmentation. However, it has been demonstrated that these tasks are very sensitive to the noise corrupting the image. While the quality of some α-tree applications has been studied, including some with noisy images, the noise impact on the whole structure has been little investigated. Thus, in this paper, we examine the structure of α-trees built on images corrupted by some noise with respect to the noise level. We compare its effects on constant and natural images, with different kinds of content, and we demonstrate the relation between the noise level and the distribution of every α-tree node depth. Furthermore, we extend this study to the node persistence under a given energy criterion, and we propose a novel energy definition that allows assessing the robustness of a region to the noise.

Keywords: α-tree · noise analysis · persistent hierarchy

1 Introduction

Hierarchical representations are powerful tools for several image processing tasks. They are divided into two categories [2]: *inclusion hierarchies* and *partitioning hierarchies*. Inclusion hierarchies describe the relation of the connected components of an image while partitioning hierarchies stack different image partitions whose regions are obtained with a given criterion. However, despite their division, there exist some links between the different categories [4]. In this article, we focus on the α-tree [14], a partitioning hierarchy. It is used for tasks such as segmentation, simplification [10], or attribute profiles [1].

To evaluate the quality of these hierarchies, a set of metrics such as the quality of regions and contours in the context of horizontal and optimal cut, is proposed and applied to hierarchical watersheds [11]. However, this evaluation does not take into account the case where a hierarchy is built on a noisy image. The impact of the noise on hierarchies applied to attribute profiles is investigated

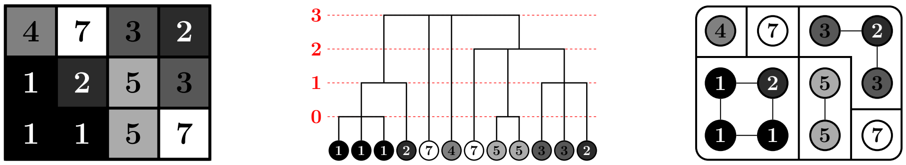

(a) An image (b) α-tree of the image (a) (c) 1-partition of (b)

Fig. 1: Illustration of the α-tree representation.

in [7], where the superiority of inclusion trees and the ω-tree compared to the α-tree is demonstrated for such applications. Finally, the α-tree structure is investigated in [15] in order to efficiently build the tree by estimating its size and only allocating the needed memory space to store the tree. Nonetheless, the impact of the noise on its structure has not been really studied.

Here, we focus on the evolution of some attributes computed on the structure of the α-trees built on images corrupted by some noise with respect to its level. The first attribute is the depth of every node in the tree, particularly their statistical distribution. The second attribute originates from the scale-set theory [5] and yields the notion of persistent nodes according to a given energy criterion. Using these attributes, we highlight the relation between the structure of the tree and the noise level, and we propose a novel energy criterion, relying on the values of a region of the tree and the gradient at its contour, in order to assert the robustness of a region to the noise.

This article is structured as follows: in Section 2, we recall the definition of the α-tree and explain how to obtain the persistence of a node when constrained to a particular energy. Then, we study the impact of the noise on the structure of the tree in Section 3. We extend this study to the node persistence in Section 4. Finally, we conclude and give the perspectives of this work in Section 5.

2 Hierarchical representations

2.1 The α-tree representation

Let $f : \Omega \to I$ be an image defined on a domain Ω and whose values belong to I. Two points $p, q \in \Omega$ are α-connected if there exists a path of m consecutive points $(p \to q) = (x_0 = p, ..., x_{m-1} = q)$ according to an adjacency relationship such that for every two consecutive points x_i and x_{i+1} of this path, $w(f(x_i), f(x_{i+1})) \leq \alpha$, with w a dissimilarity measure between two pixel values. An α-connected component is a connected component composed of α-connected points. Thus, a 0-connected component is a flat zone. An α-partition α-P is a partition composed of disjoint α-connected components whose union is Ω. An α-tree $\mathcal{T}_\alpha$ is the tree representation of the hierarchy $\mathcal{H}_\alpha = (0\text{-P}, ..., (m-1)\text{-P})$ composed of m α-partitions. Each node of $\mathcal{T}_\alpha$ represents an α-connected component and its parent represents the fusion of this node with all its siblings. Finally, a cut ζ

is a set of disjoint regions $(R_\alpha)_i$ represented by the nodes of $\mathcal{T}_\alpha$ whose union is Ω. A particular case of cut is the *horizontal cut* at a given level t which results in an α-partition with $\alpha = t$.

By applying these notions to graphs, and by the links between different hierarchical representations on edge-weighted graphs [4], the α-tree is the min-tree [13] of the minimum spanning tree of a graph, such as an adjacency graph of an image. This link leads to an efficient construction procedure based on the Kruskal algorithm [9]. Furthermore, there exist more efficient algorithms such as one based on flooding [15] or a parallel version of the α-tree construction [6].

An example of α-tree is illustrated in Fig. 1. It is built on the image in Fig. 1a and displayed in Fig. 1b as a dendrogram. In this representation, each pixel is represented by a leaf of the tree and each inner node represents the fusion of different sets of pixels. Finally, a partition of the α-tree is given in Fig. 1c.

2.2 Persistent hierarchies

Each region R of a partitioning hierarchy appears in the tree for a given continuous set of scale values associated with the hierarchy. This set is called *intervale of persistence* and is defined by $\Lambda(R) = [\lambda^+(R), \lambda^-(R)[$, where $\lambda^+(R)$ is the *scale of appearance* of R and $\lambda^-(R)$ is its *scale of disappearance*. Thus, for each region R_α represented by a node r_α of an α-tree $\mathcal{T}_\alpha$, $\lambda^+(R_\alpha)$ is the value α associated with r_α and $\lambda^-(R_\alpha)$ is the value α of the parent of r_α. The scale of disappearance of the root is a particular case where $\lambda^-(\Omega) = +\infty$.

There exist several image processing approaches relying on energy minimization for different tasks such as segmentation or denoising. Guigues *et al.* [5] propose to apply energy minimization to hierarchical representations to obtain a cut ζ^*, which is optimal according to a separable energy of the form:

$$E_\lambda(\zeta^*) = \sum_{R_i \in \zeta^*} D(R_i) + \lambda \sum_{R_i \in \zeta^*} C(R_i)$$

with $D(R_i)$ a data-fidelity term to R_i, $C(R_i)$ a regularization term and λ a parameter of this energy. When λ is varying from low value to high value, this produces different cuts whose regions are evolving from fine to coarse. Therefore, this parameter may be seen as a scale parameter, and it is possible to obtain an interval of persistence using a functional dynamic programming problem [5] by subjecting an energy of the form $E_r = D(r) + \lambda C(r)$ to a node r. This reveals some *non-persistent* nodes, with $\lambda^-(r) \leq \lambda^+(r)$, which are removed from the hierarchy, leading to a *persistent hierarchy*.

3 Noise impact on the tree structure

In the following, a noisy image is defined by $f_\sigma = f + n_\sigma$ with n_σ a sample of values drawn from a normal law $\mathcal{N}(0, \sigma^2)$. A particular case of f is the constant image f_c such that $\forall p, f_c(p) = c$, and its noisy version is denoted by $f_{c,\sigma}$. For all the experiments performed in this paper, the set of pixel values I is included or equal to $[\![0 - 255]\!]$.

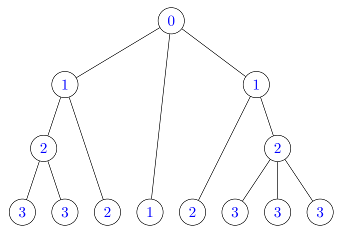

(a) Depth $\mathcal{P}_{\mathcal{T}}$ of the nodes of a tree $\mathcal{T}$

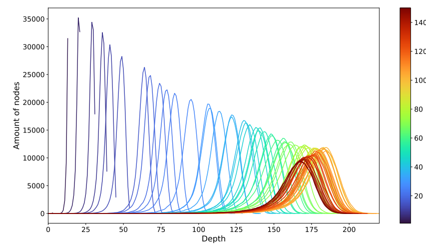

(b) Distributions $h_{c,\sigma}$

Fig. 2: The depth attribute and its representation as histograms for $f_{c,\sigma}$.

3.1 Study on a noisy constant image

We propose here to evaluate the impact of the noise on a tree $\mathcal{T}$ by studying the *depth* $\mathcal{P}_{\mathcal{T}}(r)$ of each node r, defined by

$$\mathcal{P}_{\mathcal{T}}(r) = \begin{cases} 0 & \text{if } r \text{ is the root of } \mathcal{T} \\ \mathcal{P}(r_p) + 1 & \text{else} \end{cases}$$

with r_p the parent node of r in $\mathcal{T}$. This attribute is illustrated in Fig. 2a, representing a tree whose labels in blue are the depth value of each node. The depth distribution of $\mathcal{T}$ is studied by observing its histogram h, whose values are defined by $h(d) = |\{r \in \mathcal{T} \mid \mathcal{P}_{\mathcal{T}}(r) = d\}|$ for a particular $d \in \mathcal{P}_{\mathcal{T}}$. The mode $m(h)$ of the distribution h and its empirical mean $\mu(h)$ are used throughout this paper. They are respectively obtained by $m(h) = \text{argmax}_{d \in \mathcal{P}_{\mathcal{T}}} h(d)$ and $\mu(h) = \frac{1}{|h|} \sum_{d \in \mathcal{P}_{\mathcal{T}}} h(d)$. The depth distributions obtained from the α-trees built on f_σ and $f_{c,\sigma}$ are respectively denoted by h_σ and $h_{c,\sigma}$.

In this part, the studied depth distributions are obtained from α-trees built on images containing only noise, without any texture information, in order to observe the evolution of the tree structure in the presence of noise with respect to its level. To this aim, the distributions $h_{c,\sigma}$ are built from α-trees constructed on constant images $f_{c,\sigma}$, with $c = 127$, which have been corrupted with noise whose level σ is varying from 1 to 150. The resulting distributions are displayed in Fig. 2b. The different distributions $h_{c,\sigma}$ are represented by plots whose color corresponds to the noise level σ of the image on which the α-tree is built and depicted by the color bar.

By examining these distributions, the evolution of the tree structure related to the noise level corrupting the image is studied. First, while the noise level increases, the depth distribution becomes a tailed distribution for nodes with a low depth. These nodes are α-connected components resulting from the fusion of another component and a small region, usually of size 1, which have an intensity significantly different from its surrounding pixel values. Then, the mode of the distributions increases while the noise level grows up to some high noise level, beyond which this mode decreases slowly. This is due to the clipping of values to the limits of I during the noising process of the image, creating new flat zones.

(a) Textured image

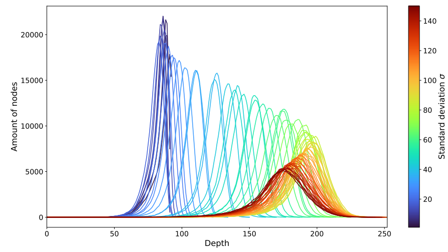

(b) Distributions h_σ for the α-tree of (a)

(c) Low brightness image

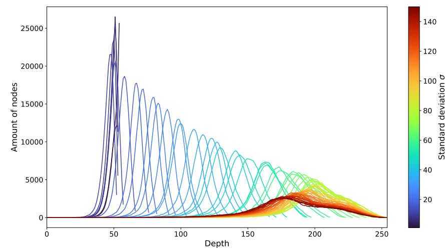

(d) Distributions h_σ for the α-tree of (c)

Fig. 3: Distributions h_σ on different kind of images.

3.2 Comparison with natural images

In this section, natural images from the database of Laurent Condat[1] are used to take into account different characteristics likely to be impacted by the noise such as a high texture or a low brightness. Examples of images are displayed in Fig. 3a and 3c, with their respective depth distributions h_σ in Fig. 3b and 3d. These distributions are obtained by the same process as previously described and using the same noise level ranges.

These distributions have similar behaviors as the ones in Fig. 2b. Their mode increases up to some noise level, and then decreases slowly. Then, the variance of each distribution is increasing as the noise level becomes high. However, there also are several differences between the distributions of tree depth obtained from $f_{c,\sigma}$ and f_σ, and between the natural images. First, the distribution modes, at low noise levels, are higher for h_σ than for $h_{c,\sigma}$. This is due to the content of the natural images which, conversely to the constant image, has some texture. Consequently, for very small σ values, the image content is still prevailing. Finally, the distributions h_σ in Fig. 3d with high σ values have a higher variance than the distributions in Fig. 3b. This demonstrates the impact of the noise on α-trees built on images with low brightness.

The analysis of the noise impact is then extended to the whole image database. For this purpose, an α-tree is built on each image and the empirical mean $\mu(h_\sigma)$ of the depth distribution h_σ is computed. This is performed

[1] https://lcondat.github.io/imagebase.html

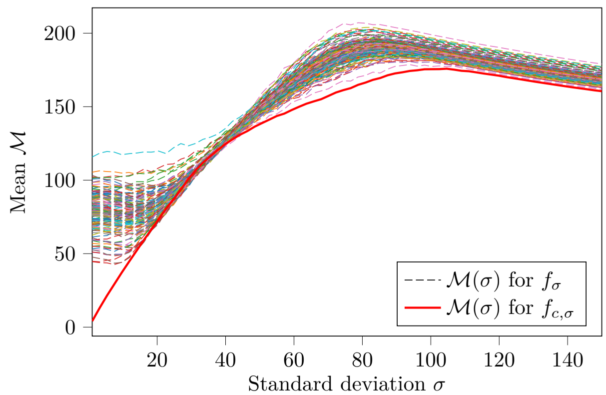

Fig. 4: Comparison between h_σ from all the images from the base and $h_{c,\sigma}$

$N = 10$ times to obtain the average $\mathcal{M}(\sigma) = \frac{1}{N}\sum_{i=0}^{N-1}\mu((h_\sigma)_i)$, with $(h_\sigma)_i$ the i^{th} depth distribution. This process is carried out for several noise levels varying between 1 and 150, resulting in the plots in Fig. 4. Each dashed plot is related to a particular image, leading to a total of 150 dashed plots. Furthermore, the red plot results from the same experiment, but with $f_{c,\sigma}$, to compare the noise impact on the structure of an α-tree built on a pure noisy image and α-trees built from images with content.

The average $\mathcal{M}(\sigma)$, at low noise levels σ, is much higher for f_σ than $f_{c,\sigma}$. This observation is true for a large majority of images in the database on every noise level. Thus, we deduce that, in spite of the noise corrupting the image, the image content has still an impact on the depth distribution of the nodes in the α-tree, as it has been observed previously. Furthermore, for every image, the values of $\mathcal{M}(\sigma)$ is decreasing starting from a given high noise level. This may come from the clipping of image values during the noising process, as previously noted for all kind of images.

4 Impact of the noise on nodes persistence

In this section, the α-trees constructed from noisy images are transformed into persistent hierarchies using a particular energy criterion. Two different energies are utilized for this purpose. First, the piecewise constant Mumford-Shah functional [8] is employed. It is defined by

$$E_{\mathrm{ms},r_\alpha}(\lambda) = \sum_{p\in R_\alpha}(f(p)-\tilde{f}(p))^2 + \lambda\,|\partial R_\alpha|$$

where $\tilde{f}$ is the average intensity of the values in the region R_α and ∂R_α is the set of elements in the contours of R_α. We propose to modify the Mumford-Shah functional to use the sum of gradient values in the contour of R_α instead of the

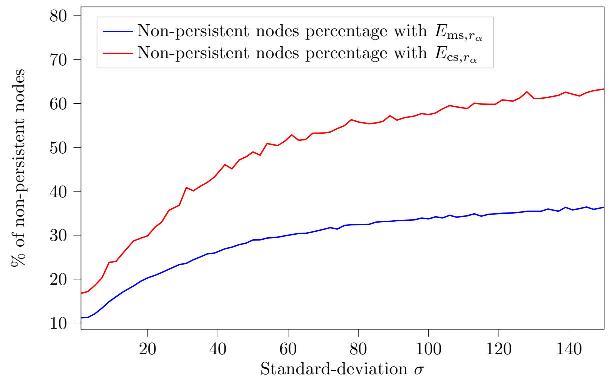

Fig. 5: Non-persistent nodes percentage related to the noise level σ

length of its contour. This functional, denoted by E_{cs,r_α}, is defined by

$$E_{\mathrm{cs},r_\alpha}(\lambda) = \sum_{p \in R_\alpha} (f(p) - \tilde{f}(p))^2 + \lambda \sum_{p \in \partial R_\alpha} g(p)$$

with g the set of contour values computed using the dissimilarity function w between two adjacent pixel values of the image from which the α-tree is built. This change of regularization term is proposed because a region with a small variance and a high gradient along its contour is most likely to be contrasted relatively to its adjacent regions, and therefore prone to be less affected by the noise in the image on which the α-tree is built.

To compare the usage of these functionals, but also to evaluate the impact of the noise on the persistence of the nodes, the percentages of non-persistent nodes using these energies E_{ms,r_α} and E_{cs,r_α} are computed on an α-tree built on the image in Fig. 3a and are displayed on Fig. 5. These plots have a similar behavior: when the noise level increases, the amount of non-persistent nodes is growing. Additionally, a greater amount of non-persistent nodes is observed when E_{cs,r_α} is used as an energy criterion than E_{ms,r_α}, and this difference is twice as large for E_{cs,r_α} at high noise levels.

The evolution of the plots of non-persistent nodes percentage is confirmed on all the images from the database with E_{ms,r_α} and E_{cs,r_α} in Fig. 6a and 6b respectively. In this figure, the average percentage of non-persistent nodes is displayed as the blue plot. Furthermore, the red line represents the percentage of non-persistent nodes on the constant image $f_{c,\sigma}$. On the two figures, the red plot has a different behavior: with E_{ms,r_α}, the amount of non-persistent nodes is close to 0%, whereas with E_{cs,r_α}, it is near 80%. This observation suggests that using E_{cs,r_α} as an energy criterion instead of E_{ms,r_α} in the presence of noise is more relevant. Furthermore, this is enforced due to the fact that when σ is increasing, the amount of non-persistent nodes on a tree built on $f_{c,\sigma}$ gets closer to the average percentage when E_{cs,r_α} is used.

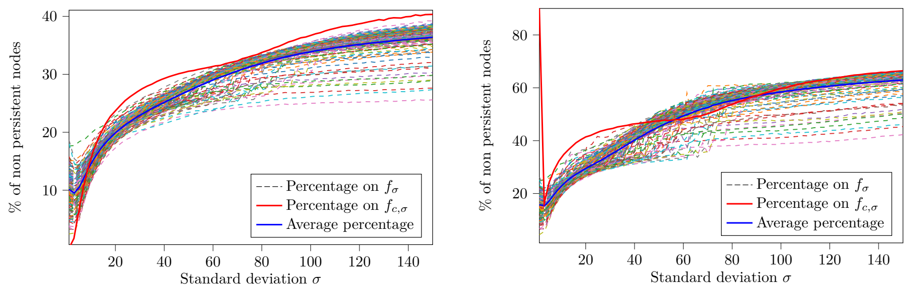

(a) With E_{ms,r_α}.

(b) With E_{cs,r_α}.

Fig. 6: Evolution of the amount of non-persistent nodes with respect to the noise level.

5 Conclusion and perspectives

To conclude this article, we have shown that there exists a relationship between the noise level degrading the image and the distribution of the depth attribute computed from the α-tree built on the noisy image. Furthermore, on natural images, we observed that the content of the image has an effect on the depth distributions: for low noise levels, the impact of noise on the α-tree is negligible, and at a high noise level, the brightness impacts the variance of the distribution. Finally, we have noticed that the choice of the functional used to obtain persistent nodes affects the amount of non-persistent nodes in the hierarchy.

We plan to extend this work to other kinds of noise, but also to generalize our study to different partitioning hierarchies such as the ω-tree [14], the binary partition trees [12], or the hierarchical watersheds [3], but also to inclusion hierarchies. Finally, we will apply the results obtained in this paper in order to evaluate the quality of hierarchies built from noisy images.

References

1. Bosilj, P., Damodaran, B.B., Aptoula, E., Mura, M.D., Lefèvre, S.: Attribute profiles from partitioning trees. In: Angulo, J., Velasco-Forero, S., Meyer, F. (eds.) Mathematical Morphology and Its Applications to Signal and Image Processing. pp. 381–392. Springer International Publishing, Cham (2017). https://doi.org/10.1007/978-3-319-57240-6˙31
2. Bosilj, P., Kijak, E., Lefèvre, S.: Partition and inclusion hierarchies of images: A comprehensive survey. Journal of Imaging **4**(2) (2018). https://doi.org/10.3390/jimaging4020033
3. Cousty, J., Najman, L.: Incremental algorithm for hierarchical minimum spanning forests and saliency of watershed cuts. In: Soille, P., Pesaresi, M., Ouzounis, G.K. (eds.) Mathematical Morphology and Its Applications to Image and Signal Processing. pp. 272–283. Springer Berlin Heidelberg, Berlin, Heidelberg (2011). https://doi.org/10.1007/978-3-642-21569-8˙24

4. Cousty, J., Najman, L., Perret, B.: Constructive links between some morphological hierarchies on edge-weighted graphs. In: Hendriks, C.L.L., Borgefors, G., Strand, R. (eds.) Mathematical Morphology and Its Applications to Signal and Image Processing. pp. 86–97. Springer Berlin Heidelberg, Berlin, Heidelberg (2013). https://doi.org/10.1007/978-3-642-38294-9˙8
5. Guigues, L., Cocquerez, J.P., Le Men, H.: Scale-sets image analysis. International Journal of Computer Vision **68**(3), 289–317 (Jul 2006). https://doi.org/10.1007/s11263-005-6299-0
6. Havel, J., Merciol, F., Lefèvre, S.: Efficient tree construction for multiscale image representation and processing. Journal of Real-Time Image Processing **16**(4), 1129–1146 (Aug 2019). https://doi.org/10.1007/s11554-016-0604-0
7. Koç, S.G., Aptoula, E., Bosilj, P., Damodaran, B.B., Dalla Mura, M., Lefevre, S.: A comparative noise robustness study of tree representations for attribute profile construction. In: 2017 25th Signal Processing and Communications Applications Conference (SIU). pp. 1–4. IEEE (2017). https://doi.org/10.1109/SIU.2017.7960159
8. Mumford, D., Shah, J.: Optimal approximations by piecewise smooth functions and associated variational problems. Communications on Pure and Applied Mathematics **42**(5), 577–685 (1989). https://doi.org/10.1002/cpa.3160420503
9. Najman, L., Cousty, J., Perret, B.: Playing with kruskal: Algorithms for morphological trees in edge-weighted graphs. In: Hendriks, C.L.L., Borgefors, G., Strand, R. (eds.) Mathematical Morphology and Its Applications to Signal and Image Processing. pp. 135–146. Springer Berlin Heidelberg, Berlin, Heidelberg (2013). https://doi.org/10.1007/978-3-642-38294-9˙12
10. Perret, B., Cousty, J., Ferzoli Guimarães, S.J., Kenmochi, Y., Najman, L.: Removing non-significant regions in hierarchical clustering and segmentation. Pattern Recognition Letters **128**, 433–439 (2019). https://doi.org/10.1016/j.patrec.2019.10.008
11. Perret, B., Cousty, J., Guimarães, S.J.F., Maia, D.S.: Evaluation of hierarchical watersheds. IEEE Transactions on Image Processing **27**(4), 1676–1688 (2018). https://doi.org/10.1109/TIP.2017.2779604
12. Salembier, P., Garrido, L.: Binary partition tree as an efficient representation for image processing, segmentation, and information retrieval. IEEE Transactions on Image Processing **9**(4), 561–576 (2000). https://doi.org/10.1109/83.841934
13. Salembier, P., Oliveras, A., Garrido, L.: Antiextensive connected operators for image and sequence processing. IEEE Transactions on Image Processing **7**(4), 555–570 (1998). https://doi.org/10.1109/83.663500
14. Soille, P.: Constrained connectivity for hierarchical image partitioning and simplification. IEEE Transactions on Pattern Analysis and Machine Intelligence **30**(7), 1132–1145 (2008). https://doi.org/10.1109/TPAMI.2007.70817
15. You, J., Trager, S.C., Wilkinson, M.H.: A fast, memory-efficient alpha-tree algorithm using flooding and tree size estimation. In: Mathematical Morphology and Its Applications to Signal and Image Processing: 14th International Symposium, ISMM 2019, Saarbrücken, Germany, July 8-10, 2019, Proceedings. pp. 256–267. Springer (2019). https://doi.org/10.1007/978-3-030-20867-7˙20